# Synthesis of Block Copolymers Containing Stereoregular Pendant Electroactive Blocks

Alexander Schmitt, Negar Kazerouni, Grace E. Castillo and Barry C. Thompson\*

**ABSTRACT:** The stereoregular non-conjugated pendant electroactive polymer (NCPEP) poly((N-carbazolylethylthio)propyl methacrylate) (PCzETPMA) has recently shown charge carrier mobilities that are on par with conjugated polymers. Here, we increased the complexity of the architecture for this NCPEP by introducing a polystyrene (PS) block via an anionic, living polymerization yielding a family of PS-b-PCzETPMA block-copolymers as the first examples of NCPEP-block-copolymers with controlled stereoregularity of the NCPEP-blocks. Through this methodology we were able to control the molar masses, PS to PCzETPMA block ratios and tacticities of the PCzETPMA-blocks. We found all three parameters to significantly impact the hole mobilities ( $\mu_h$ ) of the resulting copolymers which increased with higher molar masses, longer PCzETPMA-blocks and higher isotacticity of the PCzETPMA-block, giving the best  $\mu_h$  of 2.33 × 10 $^{\circ}$  cm<sup>2</sup>/V·s after annealing at 150 °C for the highest molar mass copolymer with a dominant isotactic PCzETPMA-block. This work is the first reported synthesis of a block-copolymer bearing a NCPEP-block with a controlled tacticity and demonstrates that such complex polymer architectures can be realized with NCPEPs while maintaining control over their stereoregularity and without significantly suppressing the hole mobility in the resulting copolymers.

Conjugated polymers (CPs) are gaining increasing attention for use in applications such as organic field-effect transistors (OFETs),¹ organic photovoltaics (OPVs),².³ organic light-emitting diodes (OLEDs),⁴ electrochromics,⁵ and bioelectronics owing to their electrochemical, optical and semiconducting properties.⁶ They offer significant advantages over their inorganic counterparts including lightweight, flexibility, low cost, biocompatibility and easy roll-to-roll processing.<sup>7,8</sup> Despite great advances, CPs still suffer from critical limitations, namely poor mechanical properties,⁴ low environmental stability,¹ low molar masses,¹¹ and limited synthetic methodologies that generally do not allow access to more complex architectures such as block copolymers.¹²

In recent years nonconjugated pendant electroactive polymers (NCPEPs) have gained interest for providing promise to overcome limitations of CPs. NCPEPs are based on a nonconjugated backbone with electroactive, pendant groups that connect to the backbone through a spacer of fixed length and nature. We note that poly(dibenzofulvene) and derivatives represent highly  $\pi$ -stacked non-conjugated polymers, albeit with limited molar mass and solubility.13 While charge carrier mobilities for NCPEPs are typically orders of magnitude lower than for CPs,14 recent work in our group has demonstrated that optimizing parameters such as the spacer length and the stereoregularity of the backbone can significantly increase hole mobilities, even outperforming the wellestablished CP poly(3-hexylthiophene) (P3HT).<sup>15-17</sup> The impact of stereoregularity on mobility in NCPEPs is analogous to the impact of regioregularity and structural regularity in general on the properties of conjugated polymers. 18,19

Past work, most notably by Thelakkat *et al.*, has further shown that hierarchically ordered structures, namely block copolymers, can be realized with NCPEPs through synthetic methodologies incompatible with traditional CPs.<sup>20</sup> While those block copolymers did not have stereoregular backbones and gave low efficiencies in OPV devices, they demonstrated a path for accessing more advanced polymer architectures.

Here we report for the first time a family of block copolymers in which one block is a stereoregular NCPEP. Poly(styrene)-b-poly(allyl methacrylate) polymers (PS-b-PAMA) with both atactic and isotactic PAMA-blocks were synthesized via living anionic polymerization and

the PAMA-block was functionalized with carbazole as the electroactive pendant group through post-polymerization functionalization. We were able to show that significant hole mobility ( $\mu_h$ ) is maintained in the functionalized block copolymers despite the introduction of an insulating PS-block and that the stereoregularity as well as the relative ratio of the electroactive PAMA-block in the copolymer heavily impacts  $\mu_h$ . This study showcases that complex polymer architectures with controlled tacticities can be realized with NCPEPs and demonstrates that desired properties such as hole mobility are maintained.

For this study block-copolymers with one electroinactive block, one electroactive block, carbazolylethylthio)propyl methacrylate) (PCzETPMA), were chosen to study how electronic properties, namely  $\mu_h$ , change when transitioning from PCzETPMA homopolymers to block-copolymers where PCzETPMA is now only making up one of the blocks as schematically shown in Figure 1. PAMA functionalized with N-Carbazolylethanethiol was chosen as the electroactive block for consistency with our study on analogous NCPEP homopolymers. 1415 The carbazole pendant groups are attached via a six-atom spacer based on our previous study on isotactic poly(N-carbazolylalkyl acrylates) reporting a six atom spacer to give the highest  $\mu_h$ . <sup>1516</sup> Introduction of the pendant group was achieved via post-polymerization functionalization of the PAMA-block in photochemical thiol-ene reactions. 1821 PS was chosen for the electroinactive block because of its well-established synthetic procedures in block-copolymers and the extensive characterization of PS (block-(co-)) polymers available in literature. 22,23

The PS-b-PAMA polymer family was synthesized via living anionic polymerization using nBuLi as the initiator (Scheme 1). Since the PS-block was meant to be atactic, higher reaction temperatures could be used than what was required for the synthesis of the stereoregular PAMA-blocks which aids in ensuring full conversion of styrene prior to addition of allyl methacrylate. Therefore, PS was chosen as the first block. Moreover, for PS, the presence of living chains can be verified through a distinct orange coloration so that it was synthetically more practical to verify the successful initiation of the PS polymerization and its transfer onto the second block. The synthesis of the PS-block was based on previous work by Hall et al. which found formation of a styrene macroinitiator from the alkyl lithium with a few drops of styrene to be a

critical step. Once the development of maximum color indicated the complete conversion of alkyl lithium to styryl anions (instantaneous in THF/toluene and after ~45minutes in toluene) the remaining styrene was added dropwise. <sup>24</sup> Molar mass and Đ for the PS-blocks (via aliquots) and detailed reaction conditions for all copolymers can be found in the supporting information.

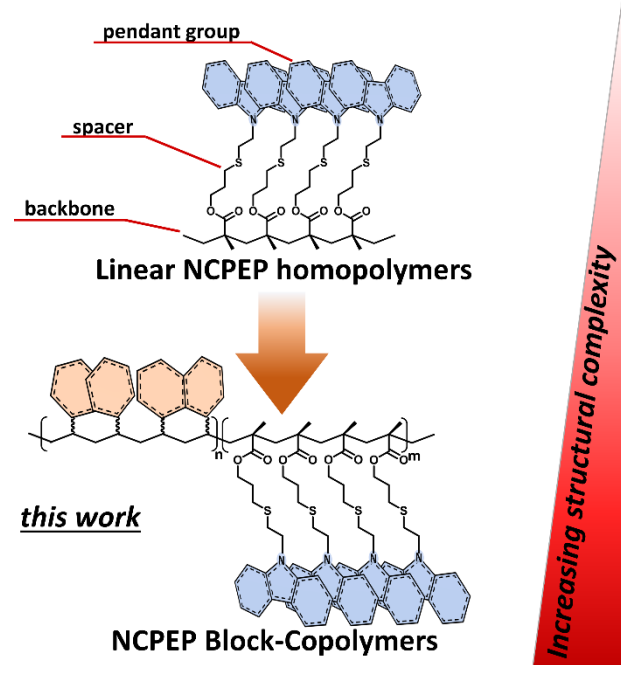


**Figure 1.** Increasing complexity of NCPEP architecture when transitioning from linear homopolymers to block-copolymers.

Synthesis of the PAMA-blocks was guided by our previous findings for stereoregular PAMA homopolymers showing that anionic polymerization in toluene at low temperatures yields highly isotactic PAMA as well as work by Brownstein *et al.* demonstrating that addition of as little as 2.5 vol-% THF to the toluene leads to atactic PAMA. <sup>15,25</sup>

Using these methods, we synthesized nine PS-*b*-PAMA block copolymers indicated as B1<sub>u</sub>-B9<sub>u</sub> (Table 1), where the subscript *u* indicates an unfunctionalized PAMA block. Here, we varied the molar mass, the tacticity of the PAMA-block and the relative ratio of the PS and PAMA blocks. As listed in Table 1, B1<sub>u</sub>-B4<sub>u</sub> are copolymers with lower molar masses ranging from 2.36-7.82 kg/mol while copolymers B5<sub>u</sub>-B9<sub>u</sub> range from 15.61-41.82 kg/mol. Table 1 also lists the block ratios for each copolymer as determined by ¹H-NMR. Additionally, the tacticity of the PAMA-blocks was controlled to give both isotactic and atactic blocks with the triad tacticities also listed in Table 1. Triad tacticities were determined from ¹H-NMR according to our previously published method for PAMA homopolymers.¹5

The PS-b-PAMA copolymers, B1<sub>u</sub>-B9<sub>u</sub>, were reacted with N-Carbazolylethanthioate under UV-irradiation ( $\lambda = 300 \text{ nm}$ ) in the of the photoinitiator 2,2-Dimethoxy-2phenylacetophenone (DMPA) affording the functionalized blockcopolymers PS-b-PCzETPMA, B1f-B9f, following our previously established post-polymerization functionalization procedure.<sup>14</sup> For B1<sub>f</sub>-B9f the subscript findicates functionalized copolymers. For the thiol-ene reaction either 1,2-dichlorobenzene or toluene were used as the reaction solvent. The choice of solvent was dictated by the solubilities of the unfunctionalized block-copolymers  $B_{1u}$ - $B_{9u}$ . As summarized in Table 1, this yielded polymers with ≥94% functionalization of the PAMA-blocks for eight out of the nine polymers. In the <sup>1</sup>H-NMR spectra, functionalization can be

followed via the disappearance of the characteristic alkene PAMA-peaks and the appearance of the aromatic peaks of the carbazole pendant group and the aliphatic spacer peaks. After functionalization with the thiol-ene reaction, all polymers were precipitated in methanol, dried, and characterized by <sup>1</sup>H NMR (see Supporting Information). The absence of sharp aromatic peaks corresponding to unreacted molecular *N*-carbazolylethanthioate indicated the effective removal of the molecular species in all cases except for B3<sub>f</sub>, where residual molecular species is likely still present (Figure S14). This is consistent with our reported results for the functionalization of PAMA homopolymers.<sup>17</sup>

While B1<sub>u</sub>-B4<sub>u</sub> copolymers with either a dominant PS or a dominant PAMA block were synthesized, it proved more difficult to realize copolymers with a dominant PAMA block in the higher molar mass range, especially under conditions required for atactic PAMA. Therefore, PS is the dominant block in B5<sub>u</sub> and B6<sub>u</sub>, however the relative ratio of the blocks was varied to range from a clearly dominant PS-block to two blocks of roughly the same length with B6<sub>u</sub>. In both B7<sub>u</sub> and B8<sub>u</sub> isotactic PAMA is the shorter block, however B7<sub>u</sub> has a significantly more dominant PS-block. For B9<sub>u</sub>, a dominant isotactic PAMA-block was achieved.

The successful formation of block copolymers was confirmed through <sup>1</sup>H-NMR and gel permeation chromatography (GPC) of aliquots of the PS-blocks and the final copolymers as well as additional control studies (vide infra). The <sup>1</sup>H-NMR spectra confirm the presence of styrene and allyl methacrylate blocks. GPC traces, which are shown in the supporting information, were used to verify the synthesis of true covalently linked block-copolymers rather than mixtures of homopolymers. Specifically, for each copolymer, GPC traces of the PSaliquot show one single peak with a positive refractive index (RI) and a very narrow D of  $\sim$ 1.20 indicative of a living polymerization. After growth of the second block, the GPC traces show a wave-shaped pattern with a negative RI associated with the PAMA block (which is consistent with previous studies on PAMA homopolymers), that immediately transitions into the PS-peak with a positive RI without leveling out on the baseline in between.<sup>15</sup> After functionalization of the PAMA-block, the copolymers show just one peak with a positive RI at a shifted molar mass compared to the PS-peak.

As an additional control study, described in depth in the supporting information, we synthesized both PS and PAMA homopolymers and made a physical mixture of the two which was stirred in boiling acetone, which is known to dissolve lower molar mass PS.<sup>26-28</sup> After filtering the solution, we found PS and small amounts of PAMA in the filtrate whereas the filtered off solids were exclusively comprised of PAMA. The same experiment with the block copolymer B9<sub>u</sub> gave no polymer in the filtrate and showed the same <sup>1</sup>H-NMR and GPC trace for the filtered off solids as before (supporting information).

All PS-b-PAMA (B1 $_u$ -B9 $_u$ ) and PS-b-PCzETPMA (B1 $_f$ -B9 $_t$ ) polymers were characterized via differential scanning calorimetry (DSC). While no significant features could be observed for the unfunctionalized copolymers or the lower molar mass functionalized polymers (B1 $_f$ -B4 $_t$ ), endothermic peaks around 75 °C and 100 °C respectively can be observed in the first cycles for B5 $_f$ -B9 $_t$  which disappear in the second cycles. These transitions are believed to stem from smectic liquid crystalline phase transitions which are known to occur within this temperature ranges for PS-block-copolymers bearing liquid crystal side-chains. <sup>29</sup> Carbazole is established to induce liquid

crystalline behavior. $^{30,31}$  No melt or crystallization transitions were observed for any copolymers.

The functionalized copolymers, both unannealed and annealed at 150 °C for 30 minutes, were further analyzed by thin-film UV-Vis absorption, showing little to no differences across the family of copolymers (supporting information) and did not show any change in features after annealing. For all functionalized samples characteristic  $\pi$ -

 $\pi^*$  transitions around 295 nm and n- $\pi^*$  transitions around 330 and 344 nm for the carbazole pendant group were observed which is consistent with what is observed for PCzETPMA homopolymers. PS homopolymers are known to exhibit an absorption band around 290 nm ascribed to the formation of intramolecular excimers. Consequently, absorption bands stemming from the PS-block in the copolymers are expected to largely coincide with the carbazole  $\pi$ - $\pi^*$  transition.  $^{32-34}$ 

Scheme 1. General synthesis of PS-b-PAMA block copolymers and functionalization with N-Carbazolylethanethioate to give PS-b-PCzETPMA.

 $Table~1.~Molar~Mass, \\ D, Yield/Conversion, \\ Triad~Tacticity~and~Block~Ratios~for~the~PS-b-PCzETPMA~Copolymers.$ 

Copolymer	M <sub>n</sub> [kg/mol]	Đ	Yield [%]a,b	Triad Tacticity [%] (mm/mr/rr)	PS:PAMA
B1 <sub>u</sub>	3.08	1.18	70ª	15/32/53	1.75 : 1
$B2_{\mathrm{u}}$	2.36	1.40	68ª	28/35/37	1:1.26
$B3_{\mathrm{u}}$	4.48	1.18	57ª	88/8/4	1.96 : 1
$B4_{\rm u}$	7.82	1.27	71ª	83/12/6	1:1.27
$\mathrm{B5}_{\mathrm{u}}$	15.61	1.14	74ª	17/23/60	1.53:1
$B6_{\mathrm{u}}$	15.98	1.19	32ª	11/30/59	1.11:1
$B7_{\rm u}$	41.82	1.14	41ª	83/10/7	3.58:1
${\bf B8}_{\rm u}$	25.93	1.24	59ª	83/13/4	1.88:1
$B9_{\rm u}$	27.55	1.21	22ª	80/11/9	1:1.22
$\mathrm{B1}_{\mathrm{f}}$	3.31	1.12	>99 <sup>b</sup>	15/32/53	1.75:1
$\mathrm{B2}_{\mathrm{f}}$	3.43	1.58	94 <sup>b</sup>	28/35/37	1:1.26
$\mathrm{B3}_{\mathrm{f}}$	4.56	1.18	>99 <sup>b</sup>	88/8/4	1.96 : 1
$\mathrm{B4}_\mathrm{f}$	10.13	1.30	>99 <sup>b</sup>	83/12/6	1:1.27
$\mathrm{B5}_{\mathrm{f}}$	16.62	1.10	97 <sup>b</sup>	17/23/60	1.53:1
$\mathrm{B6}_{\mathrm{f}}$	19.38	1.31	$90^{\rm b}$	11/30/59	1.11:1
$\mathrm{B7}_{\mathrm{f}}$	37.27	1.27	94 <sup>b</sup>	83/10/7	3.58:1
${f B8_f}$	19.96	1.25	96 <sup>b</sup>	83/13/4	1.88:1
B9 <sub>f</sub>	28.17	1.22	>99 <sup>b</sup>	80/11/9	1:1.22

Additionally, photoluminescence (PL) spectra for all annealed and unannealed functionalized copolymers were measured. The spectra for the high molar mass polymers (B5<sub>f</sub>-B9<sub>f</sub>) are shown before annealing in Figure 2a and after annealing at 150 °C for 30 minutes in Figure 2b. For all samples characteristic carbazole 0-0 transitions at 350 nm with a more sharply defined vibronic band at 370 nm were observed which match our observations on PCzETPMA homopolymers. 14,3015,33 Similarly, excimer emission peaks around 405-420 nm were absent across the entire family of copolymers as previously shown for PCzETPMA homopolymers which suggests a limited degree of  $\pi$ stacking of the pendant groups. 14,15,3215,16,35 For the unannealed low molar mass copolymers B1f-B4f (supporting information) and to a lesser degree also for B5<sub>f</sub>-B9<sub>f</sub> (Figure 2a), a broad shoulder around 400-500 nm can be seen. This feature likely stems from optical centers that are formed in the PS-blocks upon exposure to UV light, a phenomenon observed in a study on PS-homopolymer-films that found formation of fluorescing diphenylpolyene centers giving rise to fluorescence bands in the 330-520 nm region.32

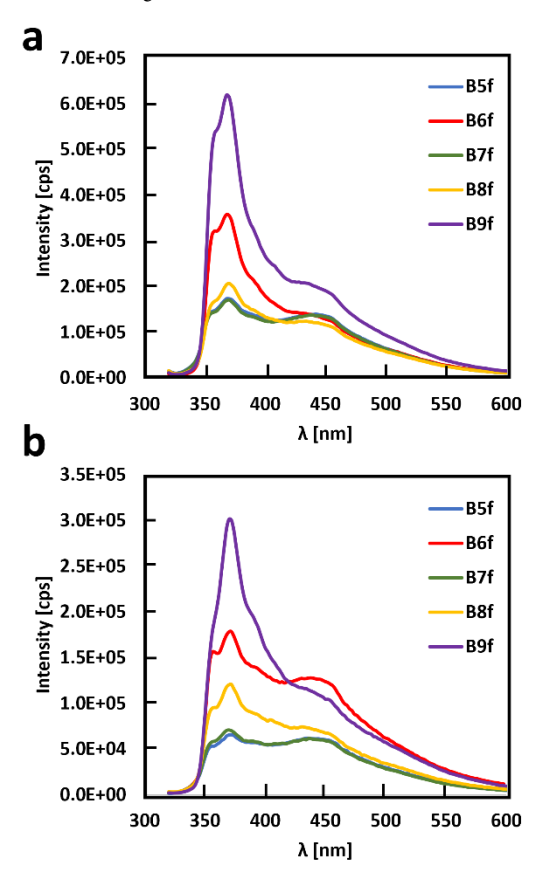


**Figure 2.** (a) PL spectra of PS-b-PCzETPMA copolymers BS<sub>f</sub>-B9<sub>f</sub> for as-cast films. (b) PL spectra of PS-b-PCzETPMA copolymers BS<sub>f</sub>-B9<sub>f</sub> after annealing at 150 °C for 30 min.

After annealing the same features in very similar relative intensities are observed with the exception of B6 $_{\rm f}$  which shows an increase in intensity for the shoulder around 400-500 nm relative to the carbazole vibronic band. PL intensities are reduced across all annealed samples implying aggregation-based PL quenching which could be indicative of a more pronounced  $\pi$ - $\pi$  stacking within the PCzETPMA-blocks in the annealed films.  $^{37,38}$ 

The space charge limited current (SCLC) technique was used to measure  $\mu_h$  for all functionalized copolymers. Measurements for each sample were repeated three times and the reported data is the average over at least 20 pixels. All copolymers were spin-coated from CHCl<sub>3</sub> and gave film thicknesses of 43-94 nm (supporting information). Based on previous studies on PCzETPMA homopolymers showing instances of significant increases in  $\mu_h$  when the polymers are annealed, SCLC was also measured after annealing at 150 °C, however, no efforts were made to optimize the annealing temperature. No significant trends were identified for samples B1<sub>f</sub>-B4<sub>f</sub>, which gave mobilities between  $1.41 \times 10^{-1}$  $^{7}$  cm $^{2}$ /V·s and 2.89 × 10 $^{-6}$  cm $^{2}$ /V·s, likely owing to the low molar masses of the four copolymers (supporting information). Comparison with B5f-B9f supports the hypothesis that molar mass has a significant influence on the mobilities of the copolymers since these higher molar mass samples show mobilities that are up to two orders of magnitude higher. The hole mobilities for unannealed and annealed copolymers B5f-B9f are depicted in Figure 3.

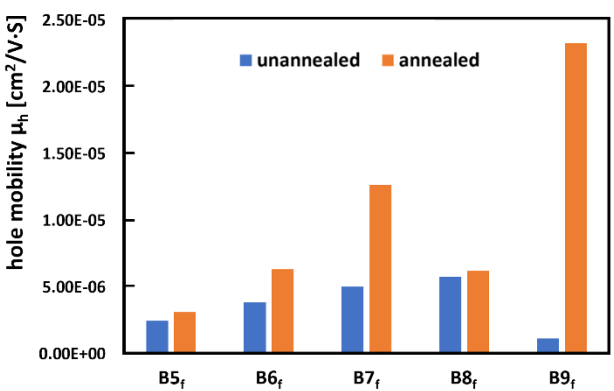


**Figure 3.** Hole mobilities of copolymers B5<sub>F</sub>B9<sub>f</sub> as cast and after annealing at 150 °C for 30 min.

For the higher molar mass samples (Figure 3) certain trends are identified. First, after annealing,  $\mu_h$  increases for all five copolymers but has a more significant effect when PCzETPMA is the dominant block as seen with B9<sub>f</sub>. Second, the stereoregularity of the PCzETPMA-block significantly impacts the relative increase in mobility after annealing upon increase of the PCzETPMA-ratio in the copolymers. Specifically, going from atactic B5f to atactic B6f the ratio of the PCzETPMA-block increases by a factor of 1.21 and a 2.02-fold increase in mobility was measured after annealing. In comparison, when going from isotactic B8<sub>f</sub> to isotactic B9f the PCzETPMA-block ratio increases by a factor of 1.6 but for the mobility a much more significant 372-fold increase was measured. Additionally, when looking at  $\mu_h$  for copolymers with comparable block-ratios that only differ in the tacticity of the PCzETPMA-block, B5f versus B8f and B6f versus B9f, the isotactic copolymers considerably outperform the atactic ones; a trend that is more pronounced when PCzETPMA is the dominant block with B9<sub>f</sub> giving a  $\mu_h$  that is higher by an order of magnitude when compared to B6<sub>f</sub>. Within the entire family of copolymers B9<sub>f</sub>, the only higher molar mass copolymer with a dominant isotactic PCzETPMA-block, gives the highest  $\mu_h$  upon annealing of  $2.33 \times 10^{-5}$  cm<sup>2</sup>/V·s which is consistent with our previous findings that higher levels of stereoregularity and higher molar masses correspond to increased  $\mu_h$  in NCPEPhomopolymers. 15,17

While the previously reported isotactic PCzETPMA homopolymer gave a superior  $\mu_h$  of  $2.19 \times 10^{-4}$  cm<sup>2</sup>/V·s upon annealing, molar mass differences between the polymers have to be considered, where  $M_n$  =

46.5 kg/mol was reported for the homopolymer and  $M_n = 28.2$  kg/mol for the copolymer (B9 $_f$ ) in this study. H15 Given the noticeable impact of molar mass on  $\mu_h$  when going from B1 $_f$ -B4 $_f$  to B5 $_f$ -B9 $_f$ , the even higher molar mass of the homopolymer could serve as one explanation for its superior mobility. Additionally, the reported homopolymer has a higher triad isotacticity of 85% compared to 80% for B9 $_f$  which likely further contributes to the higher  $\mu_h$  of the homopolymer. Interestingly, annealing of the reported homopolymer only led to a 2.7-fold increase in  $\mu_h$  while in B9 $_f$  a 19.7-fold increase was measured suggesting that achieving a favorable morphology for hole transport in the electroactive block is increasingly more dependent on thermally induced rearrangements once a second block is introduced to the polymer structure.

As an outlier, annealed B7 $_{\rm f}$  with a significantly longer PS-block than B8 $_{\rm f}$  gave a higher mobility,  $1.27 \times 10^{-5}$  cm²/V·s, compared to  $6.26 \times 10^{-6}$  cm²/V·s, indicating that PS-blocks are not just innocent bystanders but likely affect the ordering of the copolymers resulting in a more favorable morphology for hole transport. Overall, the SCLC data indicates that established principles for NCPEP homopolymers hold true. Specifically, the importance of controlling stereoregularity and achieving high molar mass to improve mobilities even when a second, electroinactive block is added to the structure. As such, having a more complex block-copolymer architecture does not significantly suppress hole mobility in cases with higher molar mass and tacticity.

In conclusion, we report a family of PS-b-PCzETPMA blockcopolymers with varied molar masses, tacticities and relative block ratios as the first examples of non-conjugated block copolymers with an electroactive block having controlled stereoregularity. Our approach allowed us to maintain control over the stereoregularity of the NCPEPblock and synthesize well-defined block-copolymers for which the relative ratios of the two blocks was tuned. Through SCLC measurements we were able to show that significant hole mobilities are maintained in the copolymers compared to PCzETPMA homopolymers. Trends previously observed in the homopolymers held true in the copolymers, most notably significant increases in hole mobility with higher molar mass and superior mobilities for stereoregular isotactic NCPEP-blocks over atactic ones with the highest molar mass copolymer featuring a dominant isotactic PCzETPMAblock, B9<sub>f</sub>, giving the best mobility of  $2.33 \times 10^{-5}$  cm<sup>2</sup>/V·s. It was also found that annealing is significantly more critical for increasing mobility in these copolymers than in homopolymers suggesting that introduction of a second block into the structure strongly affects packing of the copolymer chains. Overall, this study demonstrates that having a more complex block-copolymer architecture does not suppress hole mobility to a significant extent. This is a promising result for potential future application of pendant block-copolymers featuring multiple electroactive blocks as active materials that could allow hierarchical selforganization. Future work will center around more in-depth morphological characterization of the block copolymers.

### ASSOCIATED CONTENT

# **Supporting Information.**

Synthesis of the polymers; <sup>1</sup>H spectra; GPC and DSC traces; charge carrier mobilities; UV/Vis absorption and PL emission spectra. This material is available free of charge via the Internet at <a href="http://pubs.acs.org">http://pubs.acs.org</a>.

## **AUTHOR INFORMATION**

Corresponding Author

**Barry C. Thompson** – Department of Chemistry, Loker Hydrocarbon Research Institute, University of Southern California, Los Angeles, California 90089-1661, United States;

Email: barrycth@usc.edu

#### **Authors**

**Alexander Schmitt** – Department of Chemistry, Loker Hydrocarbon Research Institute, University of Southern California, Los Angeles, California 90089-1661, United States

**Negar Kazerouni** – Department of Chemistry, Loker Hydrocarbon Research Institute, University of Southern California, Los Angeles, California 90089-1661, United States

Grace E. Castillo – Department of Chemistry, Loker Hydrocarbon Research Institute, University of Southern California, Los Angeles, California 90089-1661, United States

#### **Author Contributions**

All authors have given approval to the final version of the manuscript.

#### Notes

The authors declare no competing financial interest.

#### **ACKNOWLEDGMENT**

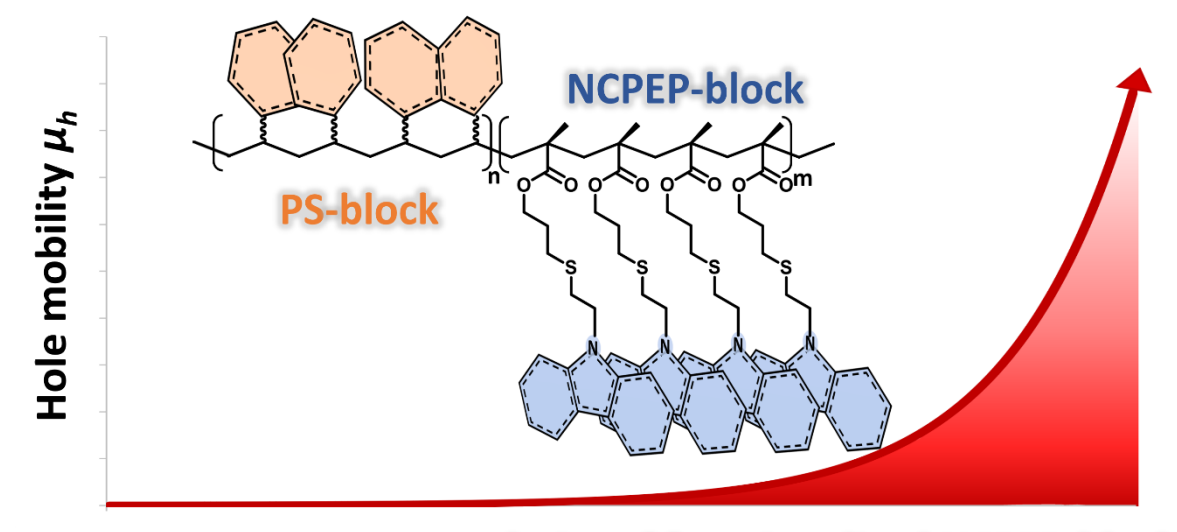
We acknowledge funding from the NSF (CHE-2106405). We acknowledge Prof. Rafael Verduzco for helpful discussions. We also acknowledge Prof. Mark E. Thompson for the use of their ellipsometer and vacuum evaporator.

# **REFERENCES**

- (1) Kim, M.; Ryu, S. U.; Park, S. A.; Choi, K.; Kim, T.; Chung, D.; Park, T. Donor-Acceptor-Conjugated Polymer for High-Performance Organic Field-Effect Transistors: A Progress Report. *Adv. Funct. Mater.* **2019**, *30* (20), 1904545.
- (2) Park, J. S.; Kim, G.-U.; Lee, S.; Lee, J.-W.; Li, S.; Lee, J.-Y.; Kim, B. J. Material Design and Device Fabrication Strategies for Stretchable Organic Solar Cells. *Adv. Mater.* **2022**, 34 (31), 2201623.
- (3) Zhang, G.; Lin, F. R.; Qi, F.; Heumüller, T.; Distler, A.; Egelhaaf, H.-J.; Li, N.; Chow, P. C. Y.; Brabec, C. J.; Jen, A. K.-Y.; Yip, H.-L. Renewed Prospects for Organic Photovoltaics. *Chem. Rev.* **2022**, *122* (18), 14180-14274
- (4) Wang, S.; Zhang, H.; Zhang, B.; Xie, Z.; Wong, W.-Y. Towards high-power-efficiency solution-processed OLEDs: Material and device perspectives. *Mater. Sci. Eng.* **2020**, *140*, 100547.
- (\$) Lo, C. K.; Wolfe, R. M. W.; Reynolds, J. R. From Monomer to Conjugated Polymer: A Perspective on Best Practices for Synthesis. *Chem. Mater.* **2021**, 33 (13), 4842-4852.
- (6) Torricelli, F.; Adrahtas, D. Z.; Bao, Z.; Berggren, M.; Biscarini, F.; Bonfiglio, A.; Bortolotti, C. A., Frisbie, C. D.; Macchia, E.; Malliaras, G. G.; McCulloch, I.; Moser, M.; Nguyen, T.-Q.; Owens, R. M.; Salleo, A.; Spanu A.; Torsi, L. Electrolyte-gated transistors for enhanced performance bioelectronics. *Nat. Rev. Methods Primers* **2021**, *1* (66).
- (7) Zhang, Z.; Liao, M.; Lou, H.; Hu, Y.; Sun, X.; Peng, H. Conjugated Polymers for Flexible Energy Harvesting and Storage. *Adv. Mater.* **2018**, *30* (13), 1704261.
- (8) Li, Z.; Chueh, C.-C., Jen, A. K.-Y. Recent advances in molecular design of functional conjugated polymers for high-performance polymer solar cells. *Prog. Polym. Sci.* **2019**, *99*, 101175.
- (9) Lu, C.; Lee, W. Y.; Gu, X.; Xu, J.; Chou, H. H.; Yan, H.; Chiu, Y. C.; He, M.; Matthews, J. R.; Niu, W.; et al. Effects of Molecular Structure and Packing Order on the Stretchability of Semicrystalline Conjugated Poly(Tetrathienoacene-Diketopyrrolopyrrole) Polymers. *Adv. Electron. Mater.* **2017**, 3 (2), 1–13.
- (10) Qiu, Z.; Hammer, B. A. G.; Müllen, K. Conjugated polymers Problems and promises. *Prog. Polym. Sci.* **2020**, *100*, 101179.

- (11) Grisorio, R.; Suranna, G. P. Intramolecular Catalyst Transfer Polymerisation of Conjugated Monomers: From Lessons Learned to Future Challenges. *Polym. Chem.* **2015**, *6* (45), 7781–7795.
- (12) Yokozawa, T.; Ohta, Y. Transformation of Step-Growth Polymerization into Living Chain-Growth Polymerization. *Chem. Rev.* **2016**, *116* (4), 1950-1968.
- (13) Nakano, T. Synthesis, structure and function of  $\pi$ -stacked polymers. *Polym. J.* **2010**, 42 (2), 103-123.
- (14) Barea, E. M.; Garcia-Belmonte, G.; Sommer, M.; Hüttner, S.; Bolink, H. J.; Thelakkat, M. Determination of Charge Carrier Mobility of Hole Transporting Polytriarylamine-Based Diodes. *Thin Solid Films* **2010**, *518* (12), 3351–3354.
- (15) Samal, S.; Schmitt, A.; Thompson, B. C. Contrasting the Charge Carrier Mobility of Isotactic, Syndiotactic, and Atactic Poly((*N*-carbazolylethylthio)propyl methacrylate). *ACS Macro Lett.* **2021**, *10* (12), 1493-1500.
- (16) Samal, S.; Thompson, B. C. Influence of Alkyl Chain Spacer Length on the Charge Carrier Mobility of Isotactic Poly(*N*-carbazolyl acrylates). *ACS Macro Lett.* **2021**, *10* (6), 720-726.
- (17) Samal, S.; Thompson, B. C. Converging the Hole Mobility of Poly(2-N-carbazoylethyl acrylate) with Conjugated Polymers by Tuning Isotacticity. *ACS Macro Lett.* **2018**, *7*, 1161-1167.
- (18) Lee, J.-W.; Sun, C.; Lee, S.-W.; Kim, G.-U.; Li, S.; Wang, C.; Kim, T.-S.; Kim, Y.-H.; Kim, B. J. Sequentially regular polymer acceptors featuring flexible spacers for high-performance and mechanically robust all-polymer solar cells. *Energy Environ. Sci.* **2022**, *15*, 4672-4685.
- (19) Kim, Y.; Park, H.; Park, J. S.; Lee, J.-W.; Kim, F. S.; Kim, H. J.; Kim, B. J. Regioregularity-control of conjugated polymers: from synthesis and properties, to photovoltaic device applications. *J. Mater. Chem. A* **2022**, *10*, 2672-2696.
- (20) Sommer, M.; Thelakkat, M. Synthesis, characterization and application of donor-acceptor block copolymer in nanostructured bulk heterojunction solar cells. *Eur. Phys. J. Appl. Phys.* **2007**, *36*, 245-249.
- (21) Roy, D.; Ghosn, B.; Song, E.H.; Ratner, D. M.; Stayton, P. S. Polymer-trimannoside conjugates *via* a combination of RAFT and thiolene chemistry. *Polym. Chem.* **2013**, *4*, 1153-1160.
- (22) Dolbey, R. *Polystyrene Synthesis, Production and Applications* 1st ed.; Wünsch, J. R.; iSmithers Rapra Publishing: Shawbury, **2000**, Vol. 10, p. 6ff.
- (23) Lynwood, C. *Polystyrene Synthesis, Characteristics and Applications* 1st ed.; Raffa, P.; Nova Science Publishers, Inc.: New York, **2014**, Vol. 1, p. 31ff.
- (24) Morton, M.; Rembaum, A. A.; Hall, J. L. Homogenous Anionic Polymerization Molecular Weight of Polystyrene Initiated by Lithium Alkyls. *J. Polym. Sci., Part A: Polym. Chem.* **1963**, *1*, 461-474.
- (25) Wiles, D. M.; Brownstein, S. Tacticity Determinations on Allyl Methacrylate Polymers. *Polym. Lett.* **1965**, *3*, 951-954.
- (26) Suh, K. W.; Clarke, D. H. Cohesive Energy Densities of Polymers from Turbidimetric Titrations. *J. Polym. Sci. Part A: Polym. Chem.* **1967**, *5*, 1671-1681.
- (27) Son, K.-S.; Jöge, F.; Waymouth, R. M. Copolymerization of Styrene and Ethylene at High Temperature with Titanocenes Containing a Pendant Amine Donor. *Macromolecules* **2008**, *41* (24), 9663-9338.

- (28) Noh, S. K.; Lee, M.; Kum, D. H.; Kim, K.; Lyoo, W. S.; Lee, D.-H. Studies of ethylene-styrene copolymerization with dinuclear contrained geometry complexes with methyl substitution at the five-membered ring in idenyl of  $[\mathrm{Ti}(\eta^5:\eta^1\text{-}C_9H_5SiMe_2NCMe_3)]_2[CH_2]_n$ . *J. Polym. Sci. Part A: Polym. Chem.* **2004**, 42 (7), 1712-1723.
- (29) Itoh, T.; Tomikawa, N.; Yamada, M.; Tokita, M.; Hirao, A.; Watanabe, J. Side-Chain Liquid Crystalline Block Copolymers with Well Defined Structures Prepared by Living Anionic Polymerization Microphase Morphology in Blends with Coil Homopolystyrenes. *Polym. J.* **2001**, 33 (10), 783-791.
- (30) Matsuura Y.; Nam, Y.; Kinoshita, M.; Ikeda T. Polarized Emission from Donor-Acceptor Liquid-Crystalline Polymers Containing Oxadiazole and Carbazole Moieties. *Mol. Cryst. Liq. Cryst.* **2009**, *513*, 153-162.
- (31) Arnim, V.; Finkelmann, H. Synthesis and phase behavior of new carbazole containing liquid crystal side chain polysiloxanes. *Macromol. Chem. Phys.* **1996**, 197, 2729-2743.
- (32) Li, T.; Zhou, C.; Jiang, M. UV absorption spectra of polystyrene. *Polym. Bullet.* **1991**, *25*, 211-216.
- (33) Uyar, T.; El-Shafei, A.; Wang, X.; Hacaloglu, J.; Tonelli, A. E. The Solid Channel Structure Inclusion Complex Formed Between Guest Styrene and Host γ-Cyclodextrin. *J. Incl. Phenom. Macrocycl. Chem.* **2006**, *55*, 109-121.
- (34) Li, M.; Bright, F. V. Steady-State Fluorescence of Polystyrene Plasticized by Supercritical Carbon Dioxide. *Appl. Spectrosc.* **1996**, *50* (6), 740-746.
- (35) Nurmukhametov, R. N.; Volkova, L. V.; Kabanov S. P. Fluorscence and Absorption of Polystyrene Exposed to UV Laser Radiation. *J. Appl. Spect.* **2006**, 73 (1), 55-60.
- (36) Healy, M. S.; Hanson J. E. Fluorescence Excitation Spectroscopy of Polystyrene Near the Critical Concentration c\*. J. Appl. Polym. Sci. 2007, 104, 360-364.
- (37) Martins, T. D.; Weiss, R. G.; Atvars, T. D. Z. Synthesis and Photophysical Properties of a Poly(Methyl Methacrylate) Polymer with Carbazolyl Side Groups. *J. Braz. Chem. Soc.* **2008**, *19* (8), 1450–1461.
- (38) Liguori, R.; Botta, A.; Pragliola, S.; Rubino, A.; Venditto, V.; Velardo, A.; Aprano, S.; Maglione, M. G.; Prontera, C. T.; De Girolamo Del Mauro, A. Study of the Electroluminescence of Highly Stereoregular Poly(N-Pentenyl-Carbazole) for Blue and White OLEDs. *Semicond. Sci. Technol.* **2017**, 32 (6), 065006.



Length and stereoregularity of functionalized NCPEP-block